Article:
Baba, Y.D., Ribeiro, J.X.F., Aliyu, A.M. et al. (2020) Characteristics of horizontal gas-liquid two-phase flow measurement in a medium-sized pipe using gamma densitometry. Scientific African, 10. e00550. ISSN: 2468-2276

https://doi.org/10.1016/j.sciaf.2020.e00550

Scientific African 10 (2020) e00550

Contents lists available at ScienceDirect

Scientific African

journal homepage: www.elsevier.com/locate/sciaf

Characteristics of horizontal gas-liquid two-phase flow measurement in a medium-sized pipe using gamma densitometry

Yahaya D. Baba[a], Joseph X.F. Ribeiro[b,*], Aliyu M. Aliyu[c], Archibong Archibong-Eso[d], Umar D. Abubakar[e], Adegboyega B. Ehinmowo[f,g]

[a] *Department of Chemical and Biological Engineering, University of Sheffield, Sheffield S1 3JD, UK*
[b] *Kumasi Technical University, P. O. Box 854, Kumasi, Ghana*
[c] *School of Computing & Engineering, University of Huddersfield, Queensgate HD1 3DH, UK*
[d] *Department of Mechanical Engineering, University of Birmingham, Dubai, UAE*
[e] *Department of Civil Engineering, Kaduna Polytechnic, Kaduna State, Nigeria*
[f] *Department of Chemical and Petroleum Engineering, University of Lagos, Akoka, Lagos, Nigeria*
[g] *Oil and Gas Engineering Centre, Cranfield University, Bedfordshire, MK43 0AL, UK*

ARTICLE INFO

Article history:
Received 7 July 2020
Revised 27 August 2020
Accepted 3 September 2020

Keywords:
Two-phase flow
Gamma densitometry
Pressure gradient
Liquid holdup and Slug flow

ABSTRACT

Two-phase flows are common occurrences in many industrial applications. The understanding of their characteristics in industrial piping systems is vital for the efficient design, optimization, and operation of industrial processes. Most of the previous experimental studies involving the use of gamma densitometers for holdup measurements in air-water mixtures are limited to smaller diameter pipes (generally regarded as those with $<$ 50 mm in nominal diameter). Further, very few literature report experimental data obtained using gamma desitometers. This paper presents an application of a gamma densitometer in the measurement of two-phase flow characteristics in an intermediate diameter pipe (nominal diameter between 50 mm and 100 mm). Scaled air-water experiments were performed in a 17-m long, 0.0764-m internal diameter horizontal pipe. Liquid superficial velocity ranged between 0.1–0.4 m/s while gas superficial velocity ranged from 0.3 to 10.0 m/s. The measured parameters include liquid holdup, pressure gradient, flow pattern, and slug flow features. The flow patterns observed were stratified, stratified-wavy, plug, slug, and annular flows. Plug and slug flow patterns showed good agreement with established flow pattern maps. Furthermore, the slug translational velocity was observed to increase with increasing mixture velocity, as reported by previous authors, hence establishing the reliability of the instrumentation employed. The slug body length was also measured using the gamma densitometer and was found to be within the range 24–36D with a mean length of 30.6D.

* Corresponding author.
E-mail addresses: y.baba@sheffield.ac.uk (Y.D. Baba), joseph.xfribeiro@kstu.edu.gh (J.X.F. Ribeiro), a.m.aliyu@hud.ac.uk (A.M. Aliyu), a.e.archibong@bham.ac.uk (A. Archibong-Eso), dahiruabubakar@kadunapolytechnic.edu.ng (U.D. Abubakar), aehinmowo@unilag.edu.ng (A.B. Ehinmowo).

https://doi.org/10.1016/j.sciaf.2020.e00550

Nomenclature

ID	Internal diameter [m]
APE	Average percentage error [%]
AAPE	Absolute average percentage error [%]
H_L	Liquid holdup [-]
I	Gamma intensity count [-]
Δl_{Gamma}	Distance between gamma densitometers [m]
SD	Standard deviation Depends on quantity
T	Time [s]
V_m	Mixture velocity [m/s]
V_{sw}	Superficial water velocity [m/s]
V_{sg}	Superficial gas velocity [m/s]
V_T	Slug translational velocity [m/s]

Introduction

Two-phase flow of liquid and gas is commonly encountered in the oil and gas industry. In most cases of normal production, co-flowing liquid and gas phases are present in pipe tubing and flow lines. In the oil and gas industry, for example, to enhance oil production or transportation, gas is often injected to lower the density and mitigate serious hydrodynamic issues, especially at junctions and elbows. When a multiphase flowing mixture is encountered, the flow characteristics are completely different from those in single-phase flow. This includes flow patterns that vary depending on the fluid properties, pipe geometry, and inclination. For oil production in harsh environments, little changes in flow characteristics become critical. The pipelines used have to be able to withstand various extreme conditions of pressure, temperature, and hydraulic issues, such as slugging, liquid surges, corrosion, and erosion. Flow assurance and transportation are heavily dependent on a sufficient understanding of flow mechanisms and related behaviours such that accurate predictions can be made.

Baker [1] developed a flow pattern map for small diameter horizontal pipes for wide range fluids mass flow rates while Mandhane et al. [2] developed flow pattern map by using phase superficial velocities as the mapping parameters for gas-liquid flows in a horizontal pipe. The classification of multiphase flow based on Gas Volume Fraction (GVF) is relevant to the instrumentation process adopted. A review of the open literature reveals that several techniques have been adopted for the measurement of two-phase flow parameters. Among the measuring principles utilised are those which employ quick-closing valves [3–5], electrical techniques [6–12], conductivity probe sensors [13–17], radial techniques [18], ultrasonic sensors [19, 20], optical techniques [21], microwave or positron emission tomography [22], wire mesh sensor [23–27], magnetic resonance imaging [28, 29], X-ray and neutron tomography [30–33]. Other researchers have developed various techniques in some practical processes for the study of two-phase flow in horizontal pipelines. One of these techniques is using invasive point sensors [34–37] such as electrical or fibre-optic probes, pitot tubes, hot wire anemometers, etc. These techniques, however, possess some disadvantages. For instance, local disturbance of the flow field constitutes one of the drawbacks.

In this study, we present detailed local measurements obtained for two-phase pressure gradient, liquid holdup, and slug flow features: slug frequency, slug liquid holdup, and slug translational velocity measured using gamma densitometers in a 0.0764-m internal diameter pipe. This is generally considered as a medium-sized pipe, and is larger than many other such studies in the literature [38–41] where pipes of 0.054-m internal diameter or less have been used. Furthermore, reported studies using gamma radiation techniques in pipes are relatively scarce, and available studies have made use of smaller pipes [42–44]. This study, therefore, presents new intermediate diameter and gamma densitometer data for the two-phase flow community for numerical model validation and facility design.

Experimental setup

Test facility description

The experimental test facility used for this study, shown schematically in Fig. 1, is located at the Cranfield University's Oil and Gas Engineering Centre. The test facility is built from a tough transparent acrylic plastic (Perspex) 3-inch pipe of about 17 m in length as depicted by a simplified diagram shown in Fig. 1. It consists of a vertical and horizontal pipe section with an observation section placed 150 pipe diameters upstream of the last injection point to ensure full development of flow in the horizontal section. The vertical section has two observation points located 100 pipe diameters from the base in both upwards and downwards pipeline. The following constitute its subsections i.e. the test fluid/material (air, water, oil, and slurry) section at injection point, unit operations equipment section, and the instrumentation and data acquisition section.

The air supply is obtained from a compressor with a maximum supply capacity of 400 m^3/hr and a discharge pressure of 7 bar. For safety and accuracy, air supply from the compressor is made to pass through a dryer and a filter to ensure the presence of moisture and particles are minimised. The flow rates are measured by two flow meters: 0.5-inch vortex flow

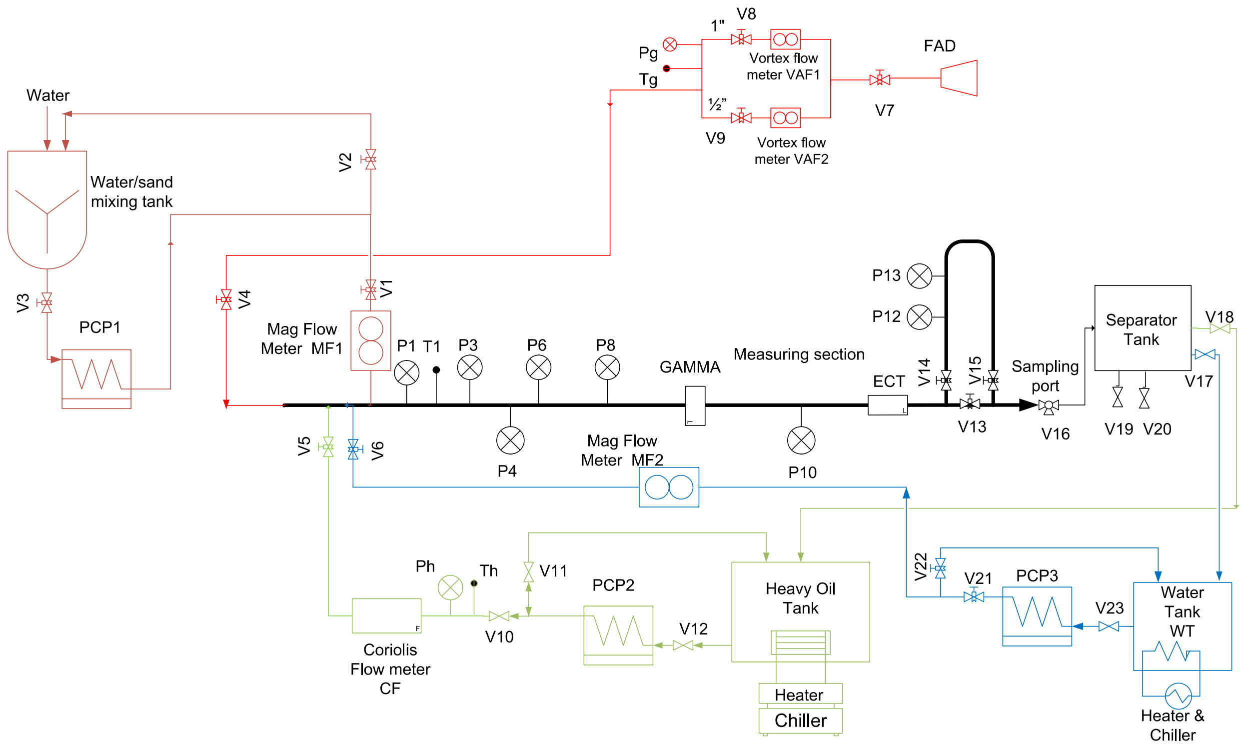

Fig. 1. Simplified flow schematic of a 3-inch pipe test facility

meter (Endress+Hauser Prowirl 72F15 DN15) with a range of 0-20 m^3/hr and a 1.5-inch vortex flow meter (Endress+Hauser Prowirl 72F40 DN40) with a range from 10-130 m^3/hr.

A 2-inch steel pipe is used to inject air into the mainline via about 150 pipe diameters upstream from the observation sections. Water, sourced from a water tap located in the laboratory and stored in a storage tank of 2 m^3, is pumped into the mainline with aid of a variable speed industrial version progressive cavity pump (PCP) with 01MR2515 model number manufactured by PCM pumps limited, the UK with a maximum speed capacity of 25 m^3/hr. The flow rate of the oil at the inlet is metered by a Coriolis flowmeter (Endress+Hauser, Promass 83F80 DN80). This flow meter with a measurement accuracy of 0.1%- 0.5% has three outputs: mass flow rate, density, and viscosity.

Experimental procedure

The procedure followed for the experimental tests starts with a visual inspection of the test facility to ensure that the facility and unit operation are in good working condition. The standard operating procedures for the facility are then followed. LabVIEW software was used for flow monitoring, entering set points, and data acquisition. The video recording cameras were set up with appropriate lighting and positioned at the observation section. A Sony HDR-CX 550 camera, wide-angle, full HD 1080 was used for the video acquisition with its lens zoomed in (or out) at the interval for each test run which lasts for 30 s.

The air compressor was first powered, and the valves set appropriately based on desired liquid and gas flow rates (in m^3/s), which were later converted to superficial velocities by dividing by the pipe cross-sectional area. The water pump suction valve and power pump are usually opened half an hour before the commencement of tests to give room for adequate circulation to achieve uniform desired viscosity with adjustment of the speed control to the desired flow rate upon start-up of the test run. Video recording and LabVIEW data acquisition were triggered to start simultaneously. Upon completion of video recording and data acquisition, the facility was shut down by safely closing the data acquisition system, oil pump, and air suction valves. The experimental test matrix used for this investigation is as follows: superficial water velocity ranges (V_{sw}) from 0.1–0.4 m/s and for each point, the superficial gas velocities (V_{sg}) used are between 0.3 and 10 m/s.

Gamma densitometers

Two single-beam gamma densitometers manufactured by Neftemer Limited, Russia, were used for the measurement of phase fractions. The key components of each gamma densitometer are highlighted in Fig. 2 above. They comprise a single energy source emitting gamma rays at 662 keV high energy level (hard spectrum) and the soft spectrum (i.e. lower en-

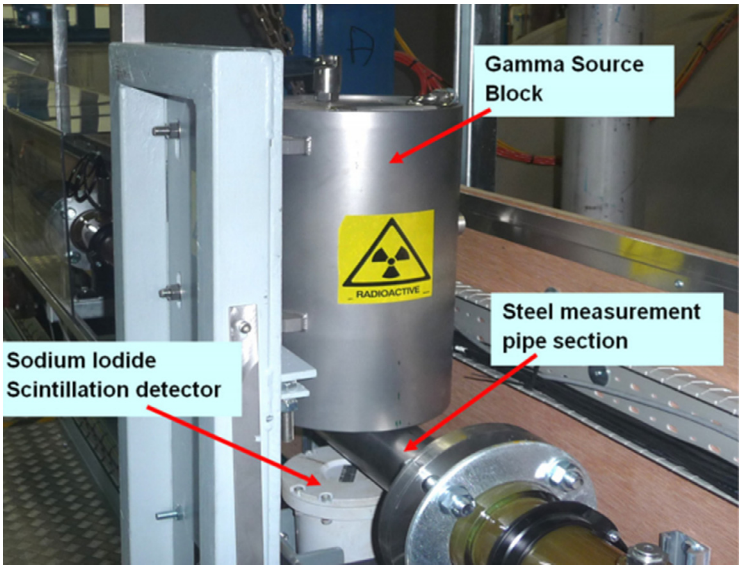

Fig. 2. Gamma-ray densitometer used for phase fraction measurement

ergy level with a range of 100~300 keV). The energy source is attenuated through a steel wall in the observation and test measurement section of the flow facility. An ICP i-7188 programmable logic controller is used to convert the raw voltage to gamma counts signals (i.e. counts are the remains of the attenuated signals upon absorption by the media it passes through).

Results and discussion

Many industrial processes (i.e. nuclear industry, refrigeration, chemical systems, and air conditioning) involve the interaction of two or more phases. The interaction of these phases results in complex mixtures and flow patterns thereby making its knowledge of great interest to facilitate better and more energy-efficient designs. Air-water tests were investigated in the 3-inch horizontal facility to benchmark the results against the existing standard and generally accepted flow pattern maps and to examine the facility's reliability as well as showcase the use of a dual gamma densitometer system in a medium diameter pipe system.

Flow pattern characterization

Visual inspections and video recordings were obtained for each flow condition during experiments. The following flow patterns were observed; stratified, stratified wavy, plug, and slug flow. The individual description of the flow patterns is presented below.

Stratified flow: This flow pattern, as illustrated (in Table 1), occurs as the dominant flow pattern at low liquid superficial velocity at V_{sw} = 0.1 m/s irrespective of the operating superficial gas velocity. It is characterized by complete separation of the two phases such that the less dense phase (gas) occupies the top of the pipe cross-sectional area while the denser phase (liquid) occupies the bottom owing to gravity effects with an undisturbed horizontal interface. This is not surprising since, as can be seen from the pictorial representation, the liquid height is not high enough to aid the transition to another flow regime.

Stratified wavy flow: Increasing the superficial gas velocity, provided the liquid height is less than half full will result in the interface becoming disturbed with surface ripples or small amplitudes illustrated in Table 1. The wave pattern has been reported to have little or no effect on the pressure fluctuations [45].

Plug flow: At a much higher liquid level and lowest gas superficial velocity, this flow regime characterized by liquid plugs with no noticeable gas entrainment and separated by elongated gas bubbles whose diameters are smaller than that of the pipe diameters are observed. Here, the elongated gas bubble is such that the phase flow in strata has the bulk of the gas at the upper periphery of the pipe while the liquid film occupies the lower periphery owing to gravity effects. Its mechanism of formation is a result of gradual build-up of the liquid level to more than half of the pipe diameter.

Slug flow: With a continuous increase in the gas velocity, a point is reached when the elongated bubble becomes similar in size as the pipe diameter moving at higher momentum with a shorter liquid body compared to plug flow. Gas entrainment is a characteristic feature of the elongated liquid body in slug flow. In comparison, however, there exists no such entrainment in plug flow.

Table 1
Observed flow patterns

V_{sw} [m/s]	V_{sg} [m/s]	Side View	Flow Pattern
0.1	0.3 -10	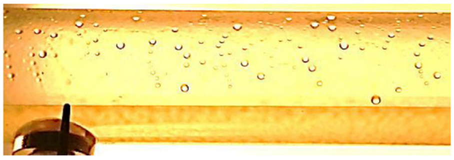	Stratified Flow
0.2- 04	0.3-0.7		Stratified-wavy flow
0.2- 04	0.7-2.0	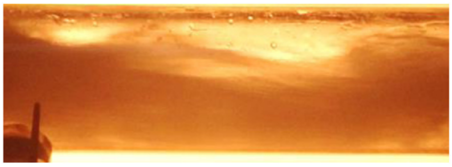	Plug Flow
0.2- 04	2.0-8.0		Slug Flow
0.2- 04	8.0-10.0		Annular flow

Annular flow: Further increasing the gas superficial velocity, a point is reached when the liquid holdup in the pipe becomes inadequate to form a liquid body capable of bridging the top of the pipe. This brings about the leftover liquid to be swept to the top section of the pipe forming an annulus liquid around the inner periphery of the pipe; thicker at the bottom owing to gravity effects with the gas phase flowing at the core of the pipe. This flow pattern is generally termed annular flow. Table 1 gives a pictorial description of the observed flow patterns.

The flow patterns observed are compared with established flow pattern maps [2, 46] as presented in Fig. 3. The choice of Beggs and Brill [46] was based on the fact that the flow pattern map was constructed over a wide range of flow condition with relatively better correlations and generally accepted in the industry while Mandhane *et al.* [2] flow pattern map was chosen because it has wide acceptability and simplicity. The test results agreed excellently with the Beggs and Brill [46] in the intermittent flow region than the Mandhane *et al.*'s [2] flow pattern map with some slight differences in the separated region which can be attributed to diameter differences yet confirming previous findings [47] which showed an increase in pipe diameter moves the transition line from separated to intermittent region towards higher liquid flow rates.

Flow pattern identification using gamma densitometer signals

Flow regime identification using the acquired gamma densitometer signals was made with signals sampled at a frequency of 250 Hz. Probability mass functions (PMF) were constructed from the time series gamma signals. The PMF structure in Fig. 4 (a) shows a bi-modal distribution with two peaks. The two-peak structure is a qualitative confirmation of visually observed intermittent flow patterns (plug and slug). The peak with the highest photon count rate is indicative of a passing film region while the smaller peak with a lower count rate is indicative of a passing slug liquid body through the detector. On the other hand, the unimodal distribution as illustrated by Fig. 4 (b) is indicative of annular flow.

Liquid holdup

Liquid holdup plays a very vital role in the oil and gas industry as its accurate prediction is crucial to the effective prediction of many two-phase flow calculations and in most cases serves as the starting point for these predictive models.

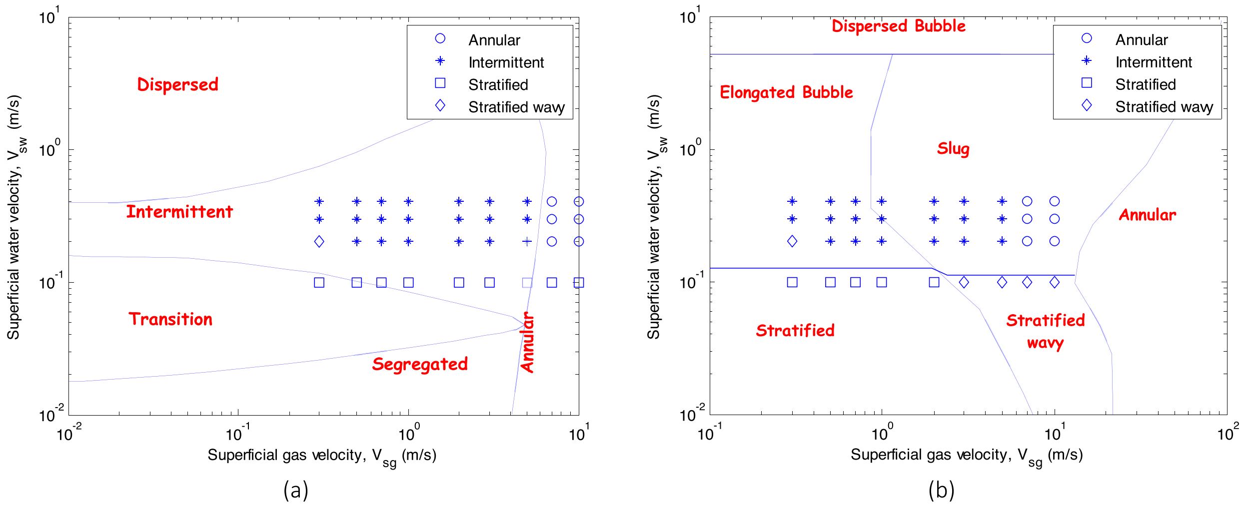

Fig. 3. Comparison of air-water test and (a) Beggs and Brill (1973) flow pattern map (b) Mandhane et al. (1974) flow pattern map

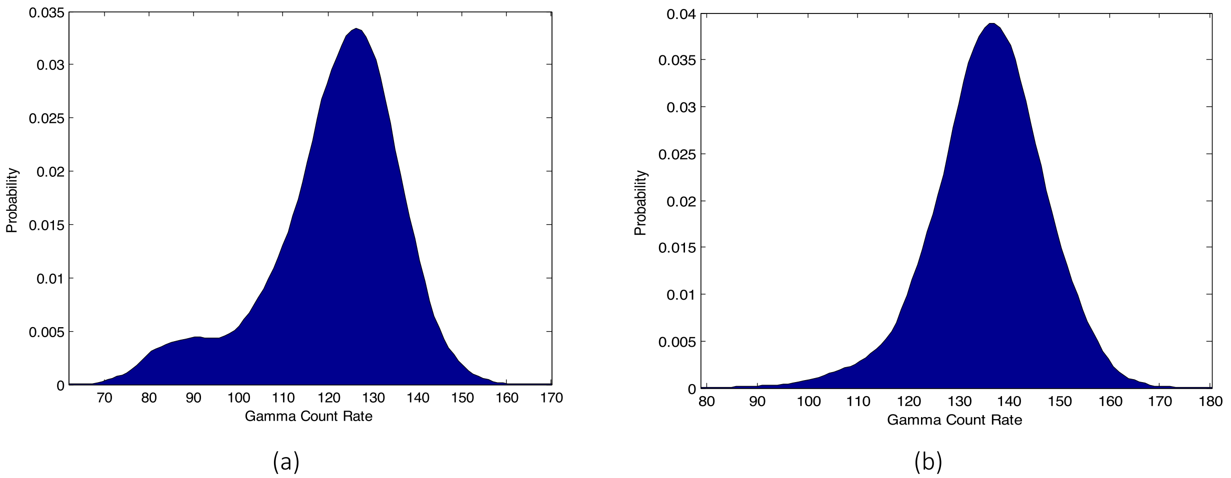

Fig. 4. Sample plots of probability mass function of hard gamma count rates used for slug and annular flow regime identification for the air-water experiments respectively (a) $\boldsymbol{V_{sw}}$ = 0.2 m/s, $\boldsymbol{V_{sg}}$ = 1.0 m/s (b) $\boldsymbol{V_{sw}}$ = 0.2 m/s, $\boldsymbol{V_{sg}}$ = 9.0 m/s

The experimental liquid holdup was computed from gamma densitometer photon count using the Beer-Lambert logarithmic equation:

$$H_L = \left[ln\left(\frac{I_M}{I_A}\right) / ln\left(\frac{I_L}{I_A}\right) \right] \quad (1)$$

where I_M = average gamma count obtained from the liquid-gas mixture in the pipe, I_A = average calibration gamma data obtained for empty pipe (i.e.100% Air), I_L= average calibration gamma data obtained for pipe containing pure liquid and H_L= Liquid holdup. The result of the liquid holdup as presented in Fig. 5 shows the time-averaged liquid holdup measurement obtained for 30 sec exhibits a general decreasing trend for liquid holdup value as the gas superficial velocity increases. An increase in the gas superficial velocity brings about more of the gas phase occupying the total cross-sectional area of the pipe analogous to the reduction of the liquid holdup in the cross-section area of the pipe. Error bars shown on the plots were obtained as a result of conducting a set of triplicate tests to ascertain repeatability and quantify the level of uncertainty. It was found that repeated tests deviated at an average of ±8% from each other and this informed the magnitude of error bars placed on the liquid holdup measurements.

Slug translational velocity

Slug translational velocity is one of the closure parameters often utilized as an input parameter for most slug flow models. Here, it was experimentally estimated by dividing the distance between the two gamma densitometers by the time lag

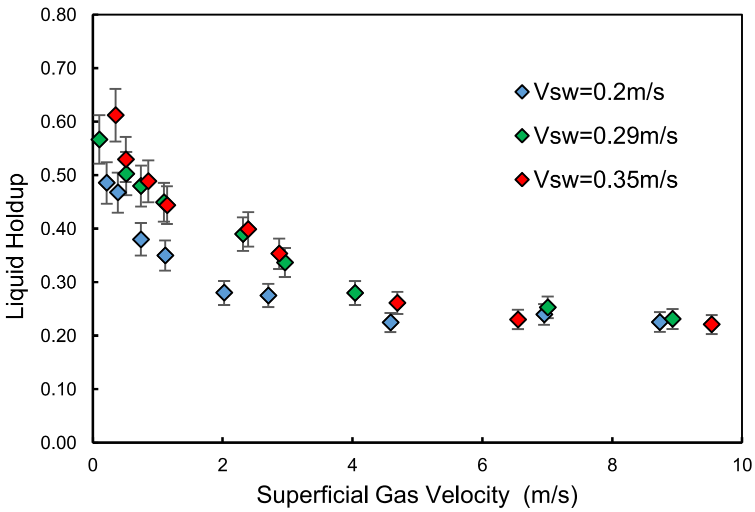

Fig. 5. Measured Liquid Holdup versus Superficial Gas Velocity

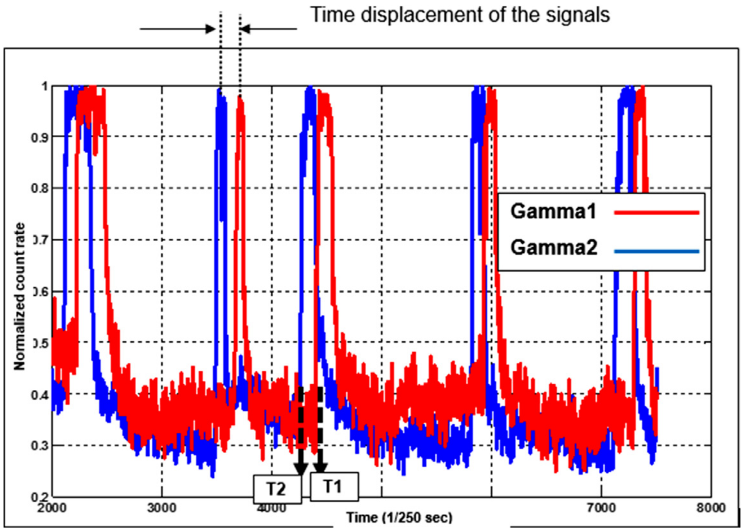

Fig. 6. Liquid holdup time trace for the two Gamma densitometer used

obtained from the cross-correlation of the signal output from the gamma densitometer. Analysis of the holdup time series result obtained from two gamma densitometers located at 103D and 124D downstream of the water injection point were utilized for translational velocity data collection as depicted in Fig. 6. For this investigation, noisy signals associated with such phenomena were minimized by using signal filters in MATLAB (i.e. the “smooth” function).

From Fig. 6, the distance between the two gamma densitometers is given as Δl_{Gamma} and the arrival times of the slug front at first and second densitometer are denoted by T_1 and T_2 respectively. However, for fast-sampled data with large signal lengths, manual peak to peak time lag identification is not practical and an algorithm was written using MATLAB’s signal processing toolbox to do this. Cross-correlation is a standard method for measuring the degree of matching between two signals to determine the time difference that exists between them. This was implemented on the two-gamma densitometer signal time series as presented. The cross-correlation function for two-time series $a(t)$ and $b(\tau - t)$ is given as

$$C_{ab}(\tau) = \frac{1}{N} \int_{-\infty}^{\infty} a(t)\ \mathrm{b}(\tau - t)\mathrm{d}t \tag{2}$$

where τ is the temporal lag. For two discrete signals, $a(t_n)b(\tau - t_n)$, where $n = 1, 2, 3, \ldots, N$, sampled at an equal time interval, the cross-correlation coefficient is given as a summation rather than an integral:

$$C_{ab}(\tau) = \frac{1}{N} \sum_{n=1}^{N} a(t_n)\ \mathrm{b}(\tau - t_n) \tag{3}$$

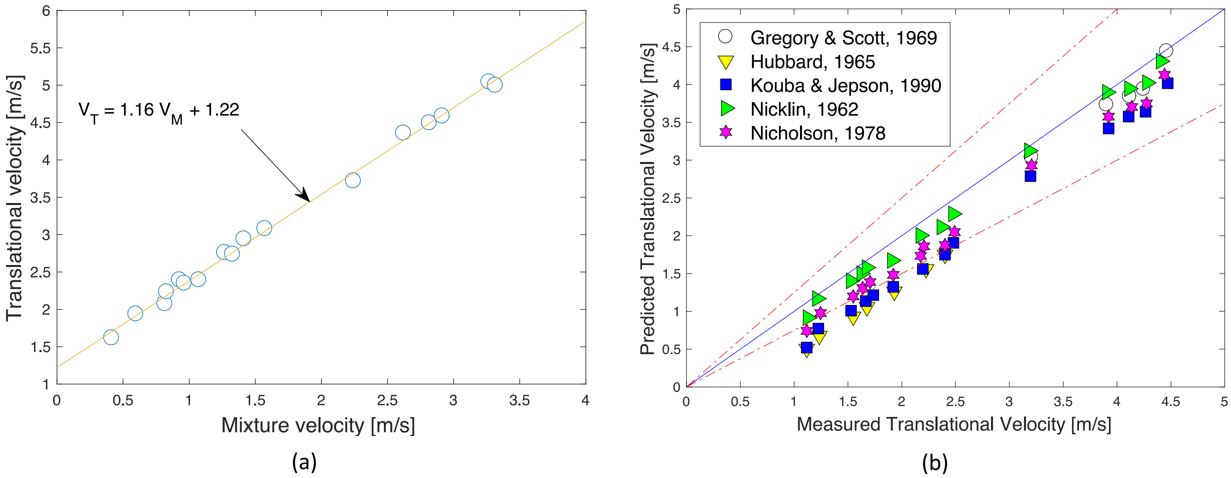

Fig. 7. (a) Slug translational velocity plotted as a function of mixture velocity (b) Comparison between slug translational velocity measured data and prediction models

Table 2
Performance evaluation of prediction models for present data

Prediction Model	APE	AAPE	SD
Nicklin [59]	-6.58	6.58	4.31
Gregory and Scott [53]	-20.92	20.92	15.81
Hubbard [54]	-26.78	26.78	14.64
Kouba & Jepson [55]	-23.36	23.36	11.50
Nicholson *et al.* [56]	-16.57	16.57	8.07

This can be plotted as a distribution of time intervals τ_n, such that the most probable time interval is that with the distinct highest peak of the cross-correlation coefficient C_{ab}. Thus, the slug translational velocity is calculated using this most probable time interval as follows:

$$V_T = \frac{\Delta l_{Gamma}}{T_1 - T_2} = \frac{\Delta l_{Gamma}}{\tau} \tag{4}$$

where Δl_{Gamma} is the distance between the two gamma densitometers. Presented in Fig. 7 (a) is measured slug translational velocity plotted as a function of mixture velocity, and this indicates a linear tendency such that slug translational velocity increases as mixture velocity increases for all the flow conditions investigated. The observed trend is consistent with previous findings [48–51].

Evaluation of slug translational velocity and models

Measured slug translational velocity in this study was compared with prediction models in the literature [52–56]. The performance evaluation as presented in Fig. 7 (b) and Table 2 shows that Nicklin *et al.* [52] and Nicholson *et al.* [56] give better agreement with the present data as compared to others. Models for slug translational velocity and their model parameters have been comprehensively compiled and given in the study by Baba *et al.* [57]. This can be attributed to the fact that they both accounted for drift velocity which has been shown [56, 58] to exist in horizontal cases and can even exceed the vertical case value.

Slug body length

This closure parameter is another primary variable in slug flow modelling. It was estimated by multiplying the obtained translational velocity by the time lag for the flow conditions investigated. The result shows the measured slug body length is in the region of 24-36D with a mean length of 30.6D and agrees with the work of Pan [50]. He observed an approximate length of 20-40D and a mean length of 30D for air-water and 24D for 4cP oil-air experiment in a 0.075 m ID pipe as presented in Fig. 8 showing measured slug length plotted as a function of mixture velocity. Other experimental observations [56, 60–62] for air-water in both upward vertical and horizontal flow systems suggest that the average stable liquid slug length is relatively insensitive to the gas and liquid flow rates.

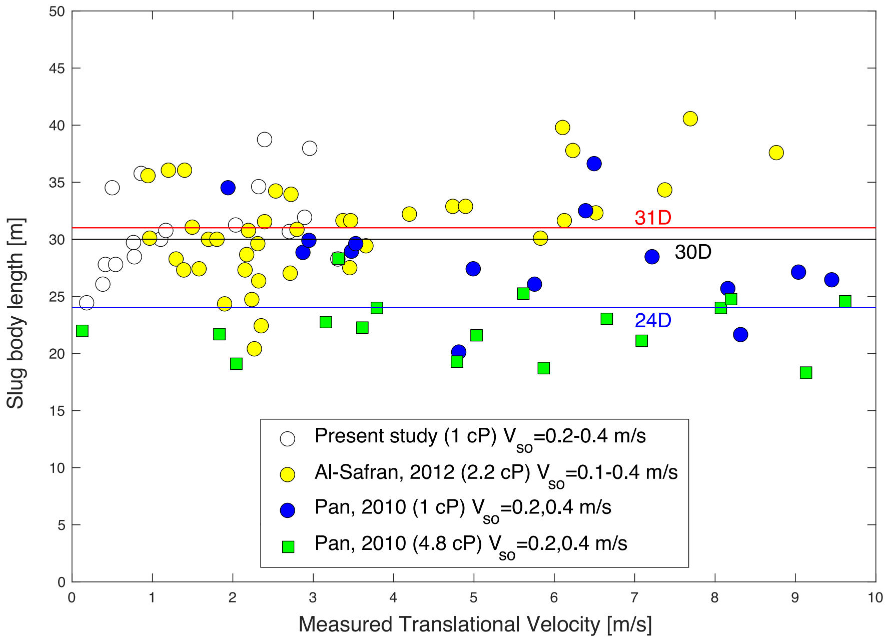

Fig. 8. Slug length as a function of mixture velocity

Table 3
Evaluation of slug length prediction against present data

Prediction Model	APE	AAPE	SD
Norris [65]	-78.07	78.07	3.31
Brill *et al.* [66]	-70.90	70.90	3.43
Gordon and Fairhurst [67]	4109.47	4109.47	495.63
Scott *et al.* [68]	811.99	811.99	137.48

However, they noted the lengths are dependent mainly on the pipe diameter. They also concluded that the mean slug lengths are in the range of 15-40D. We found our slug lengths to be lognormally distributed, agreeing with the findings of Nydal *et al.* [63]. The authors carried out statistical distributions of slug characteristics in the air-water two-phase flow horizontal system for which they concluded that the cumulative probability density function of measured slug length right-skewed and fits a log-normal distribution.

Gamma readings were acquired at an average measurement time of 70 seconds for each experimental run. It is estimated that the entire sources of error in slug length measurement result in a maximum of ±5% uncertainty by the gamma densitometers. These errors include systematic errors in the Sodium Iodide (NaI) scintillation radiation by the densitometer detector and errors that arise from time-varying fluctuations of the two-phase flow in the measurement cross-section. The measured slug body length was compared with available slug body length prediction models in the literature. A comprehensive summary of slug length correlations and their model parameters has been comprehensively compiled and reported by Baba et al. [64]. Those whose performances were evaluated [65–68] are as shown in Table 3. The prediction models of Norris [65] and Brill *et al.* [66] are closer and performed better when compared to Gordon and Fairhurst [67]; Scott *et al.* [68] and this is not surprising since Norris [65] is a modified version of Brill *et al.* [66] by the exclusion of the mixture velocity term which was found to be negligible. Gordon & Fairhurst [67] and Scott *et al.* [68] exhibited very high discrepancy which can be attributed to the fact that both correlations were regressed from very large large-diameter oil and gas transportation pipelines where there is the possibility of long terrain-induced slugs.

Conclusion

An experimental air-water two-phase flow study has been conducted using a gamma radiation technique with two densitometers that measure slug flow characteristics. Liquid holdup and slug translational velocity measurements were carried out on a 0.074-m ID horizontal test facility. Flow patterns for the experiments conducted were identified using a combination of visual observation and statistical analysis of hard gamma counts of the various flow conditions. The flow patterns observed were stratified, stratified-wavy, plug, slug, and annular flows. A comparison of observed flow patterns with established flow pattern maps shows a good agreement for the dominating flow pattern (plug and slug flow pattern). Also, measurement of slug translational velocity and slug body length were carried out. Measured slug translational velocity plotted as a function of mixture velocity shows an increase in the translational velocity with increasing mixture velocity conforming to the findings of earlier researchers using smaller diameter pipes. Also measured was the slug body length which was found to be 24-36D with a mean length of 30.6D. The obtained result agrees with various postulations in the literature. Conclusively, this study generally demonstrates the reliability of the test facility and instrumentation used.

Funding

The authors received no funding for this work.

Declaration of Competing Interest

The authors declare that they have no known competing financial interests or personal relationships that could have appeared to influence the work reported in this paper.

References

[1] D. Baker, Simultaneous flow of oil and gas, Oil Gas J. 153 (1954) 183–195.
[2] J.M. Mandhane, G.A. Gregory, K. Aziz, A flow pattern map for gas-liquid flow in horizontal pipes, Int. J. Multiph. Flow 1 (4) (1974) 537–553.
[3] J.X.F. Ribeiro, et al., An assessment of gas void fraction prediction models in highly viscous liquid and gas two-phase vertical flows, J. Nat. Gas Sci. Eng. 76 (Apr. 2020) 103107.
[4] J.X.F. Ribeiro, R. Liao, A.M. Aliyu, Z. Liu, Prediction of pressure gradient in two and three-phase flows in vertical pipes using an artificial neural network model, Int. J. Eng. Technol. Innov. 9 (3) (2019) 155–170.
[5] J.X.F. Ribeiro, R. Liao, A.M. Aliyu, Z. Liu, Upward interfacial friction factor in gas and high-viscosity liquid flows in vertical pipes, Chem. Eng. Commun. 207 (9) (2020) 1234–1263.
[6] C.G. Xie, et al., Electrical capacitance tomography for flow imaging— system for development of image-reconstruction algorithms and design of primary sensors, IEE Proc. G 139 (1992) 89–98.
[7] S. F. A. Bukhari and W. Q. Yang, “Tomographic imaging technique for oil separator control,” in 3rd International Symposium on Process Tomography, 2004, pp. 27–31.
[8] L. Zhang, H. Wang, Identification of oil-gas two-phase flow pattern based on SVM and electrical capacitance tomography technique, Flow Meas. Instrum 21 (1) (2010) 20–24.
[9] M. J. Da Silva, Impedance sensors for fast multiphase flow measurement and imaging. 2008.
[10] J. Jia, M. Wang, H.I. Schlaberg, H. Li, A novel tomographic sensing system for high electrically conductive multiphase flow measurement, Flow Meas. Instrum. 21 (3) (2010) 184–190 Sep..
[11] J.Z. Wang, G.Y. Tian, G.P. Lucas, Relationship between velocity profile and distribution of induced potential for an electromagnetic flow meter, Flow Meas. Instrum. 18 (2007) 99–105.
[12] L.F.. Jeanmeure, T. Dyakowski, W.B.. Zimmerman, W. Clark, Direct flow-pattern identification using electrical capacitance tomography, Exp. Therm. Fluid Sci. 26 (6–7) (2002) 763–773 Aug..
[13] A.M. Aliyu, A.A. Almabrok, Y.D. Baba, L. Lao, H. Yeung, K.C. Kim, Upward gas–liquid two-phase flow after a U-bend in a large-diameter serpentine pipe, Int. J. Heat Mass Transf. 108 (2017) 784–800 May.
[14] S. Kim, X.. Fu, X. Wang, Study on interfacial structures in slug flows using a miniaturized four-sensor conductivity probe, Nucl. Eng. Des. 204 (2001) 45–55.
[15] A.M. Aliyu, L. Lao, A.A. Almabrok, H. Yeung, Interfacial shear in adiabatic downward gas/liquid co-current annular flow in pipes, Exp. Therm. Fluid Sci. 72 (2016) 75–87.
[16] A.M. Aliyu, et al., Prediction of entrained droplet fraction in co-current annular gas–liquid flow in vertical pipes, Exp. Therm. Fluid Sci. 85 (2017).
[17] A.A. Almabrok, A.M. Aliyu, L. Lao, H. Yeung, Gas/liquid flow behaviours in a downward section of large diameter vertical serpentine pipes, Int. J. Multiph. Flow 78 (2016) 25–43.
[18] F. Fischer, U. Hampel, Ultra fast electron beam X-ray computed tomography for two-phase flow measurement, Nucl. Eng. Des. 240 (2010) 2254–2259.
[19] R.D.. Carvalho, O.. Venturini, E.. Tanahashi, Application of the ultrasonic technique and high-speed filming for the study of the structure of air–water bubbly flows, Exp. Therm. Fluid Sci. 33 (2009) 1065–1086.
[20] S. Al-lababidi, D. Mba, A. Addali, Upstream multiphase flow assurance monitoring using acoustic emission, Acoust. Emiss. (2012) 398.
[21] F. Murzyn, D. Mouaze, J. Chaplin, Optical fibre probe measurements of bubbly flow in hydraulic jumps, Int. J. Multiph. Flow 31 (2005) 141–154.
[22] Z. Wu, Developing a microwave tomographic system for multiphase flow imaging: advances and challenges, Trans. Inst. Meas. Control 37 (2015) 760–768.
[23] P.V. Hernandez, Gas-liquid two-phase flow in inclined pipes, PhD Thesis, University of Nottingham, 2007.
[24] A.M. Aliyu, et al., Prediction of entrained droplet fraction in co-current annular gas–liquid flow in vertical pipes, Exp. Therm. Fluid Sci. 85 (2017) 287–304 Jul..
[25] I. Johnson, “Method and apparatus for measuring water in crude oil,” US4644263A, 13-Dec-1984.
[26] N. Reinecke, G. Petritsch, M. Boddem, Tomographic imaging of the phase distribution in two-phase slug flow, Int. J. Multiph. Flow 24 (1998) 617–634.
[27] A.A. Almabrok, A.M. Aliyu, Y.D. Baba, L. Lao, H. Yeung, Void fraction development in gas-liquid flow after a U-bend in a vertically upwards serpentine–configuration large-diameter pipe, Heat Mass Transf. und Stoffuebertragung 54 (1) (2018) 209–226.
[28] E. Fukushima, Nuclear magnetic resonance as a tool for multiphase metering, Annu. Rev. Fluid Mech. 31 (1999) 95–123.
[29] D.. Holland, A. Blake, A.. Taylera, J. Sedermana, and L.. Gladdena, “Bayesian design of magnetic resonance studies of multiphase flows experimental methods for multiphase flows.,” in 7th International Conference on Multiphase Flow - ICMF, 2010.
[30] M. Al-Wadahi, A. Grader, An investigation of three-phase counter-current flow using X-ray computerized tomography and neuro-simulation modeling, SPE Annu. Tech. 1 (1) (2000) 15–20.
[31] R. F. Mudde, “Fast X-Ray tomography of a bubbling fluidized bed,” 13th Int. Conf. Fluid. New Paradig. Fluid. Eng., 2010.
[32] H. Prasser, M. Misawa, I. Tiseanu, Comparison between wire-mesh sensor and ultra-fast X-ray tomograph for an air–water flow in a vertical pipe, Flow Meas. Instrum. 16 (2005) 73–83.
[33] U. Hampel, et al., Application of gamma tomography to the measurement of fluid distributions in a hydrodynamic coupling, Flow Meas. Instrum. 16 (2–3) (2005) 85–90.
[34] D. Barnea, A unified model for predicting flow-pattern transitions for the whole range of pipe inclinations, Int. J. Multiph. Flow 13 (Jan. 1) (1987) 1–12.
[35] F.L. Hau, S. Banerjee, Measurement of mass flux in two-phase flow using combination of pitot tubes and gamma densitometers, AIChE J. 27 (1981) 177–184.
[36] R. Manabe, T. Tochikawa, O. Corp, M. Tsukuda, N. Arihara, U. Waseda, Experimental and modeling studies of two phase flow in pipelines, J. SPE Prod. Facil. 12 (1997) 212–217 November.

[37] J. Weisman, D. Duncan, J. Gibson, T. Crawford, Effects of fluid properties and pipe diameter on two- phase flow patterns in horizontal lines, Int. J. Multiph. Flow 5 (6) (1979) 437–462.
[38] R.V.A. Oliemans, B.F.M.F.M. Pots, N. Trompé, Modelling of annular dispersed two-phase flow in vertical pipes, Int. J. Multiph. Flow 12 (5) (Sep. 1986) 711–732.
[39] N.K. Omebere-Iyari, B.J. Azzopardi, A study of flow patterns for gas/liquid flow in small diameter tubes, Chem. Eng. Res. Des. 85 (2) (2007) 180–192.
[40] G. H. Anderson and P. D. Hills, "Two-phase annular flow in tube bends," in Symposium on Multiphase Flow Systems, 1974.
[41] T. Oshinowo, M.E. Charles, Vertical two-phase flow part I. Flow pattern correlations, Can. J. Chem. Eng. 52 (1) (1974) 25–35 Feb..
[42] Y. Jiang, K.S. Rezkallah, An experimental study of the suitability of using a gamma densitometer for void fraction measurements in gas-liquid flow in a small diameter tube, Meas. Sci. Technol. 4 (4) (1993) 496–505 Apr..
[43] A.M.C. Chan, S. Banerjee, Design aspects of gamma densitometers for void fraction measurements in small scale two-phase flows, Nucl. Instruments Methods Phys. Res. 190 (1) (1981) 135–148.
[44] Y. Zhao, Q. Bi, R. Hu, Recognition and measurement in the flow pattern and void fraction of gas–liquid two-phase flow in vertical upward pipes using the gamma densitometer, Appl. Therm. Eng. 60 (Oct. 1–2) (2013) 398–410.
[45] R. Kaji, B.J. Azzopardi, The effect of pipe diameter on the structure of gas / liquid flow in vertical pipes, Int. J. Multiph. Flow 36 (4) (2010) 303–313.
[46] U. Beggs, U. D.H., J.P. Brill, A study of two-phase flow in inclined pipes, J. Petrol. Technol. 25 (5) (1973) 607–617.
[47] J. Weisman, D. Duncan, J. Gibson, T. Crawford, Effects of fluid properties and pipe diameter on two-phase flow patterns in horizontal line, Int. J. Multiph. Flow 5 (1979) 437–462 no. C.
[48] E. Carpintero Rogero, Experimental investigation of developing plug and slug flows, Doctoral Thesis., TECHNISCHE UNIVERSITÄT MÜNCHEN, 2009.
[49] C. H. Romero, M. A. Márquez, S. D. Vergara, and M. T. Valecillos, "Experimental determination of hydrodynamic parameters of air-water two-phase slug flow in horizontal pipes," in Proceedings of the ASME 2012 Fluids Engineering Summer Meeting, 2012.
[50] J. Pan, Gas entrainment in two-phase gas-liquid slug flow, PhD Thesis, Imperial College London, 2010.
[51] M. Lu, "Experimental and computational study of two-phase slug flow," Imperial College London, 2015.
[52] D. Nicklin, J. Wilkes, J. Davidson, Two phase flow in vertical tubes, Trans. Inst. Chem. Eng. 40 (1962) 61–68.
[53] G.A. Gregory, D.S. Scott, Correlation of liquid slug velocity and frequency in horizontal cocurrent gas-liquid slug flow, AIChE J. 15 (6) (1969) 933–935.
[54] M. G. Hubbard, "An analysis of horizontal gas-liquid slug flow," University of Houston, 1965.
[55] G.E. Kouba, W.P. Jepson, The flow of slugs in horizontal, two-phase pipelines, J. Energy Resour. Technol. 112 (1) (1990) 20 Mar..
[56] M.K. Nicholson, K. Aziz, G.A. Gregory, Intermittent two phase flow in horizontal pipes: predictive models, Can. J. Chem. Eng. 56 (6) (1978) 653–663 Dec..
[57] Y.D. Baba, et al., Slug translational velocity for highly viscous oil and gas flows in horizontal pipes, Fluids 4 (3) (2019).
[58] K.H. Bendiksen, An experimental investigation of the motion of long bubbles in inclined tubes, Int. J. Multiph. Flow 10 (4) (1984) 467–483 Aug..
[59] D.J. Nicklin, Two-phase bubble flow, Chem. Eng. Sci. 17 (9) (1962) 693–702 Sep..
[60] A.E. Dukler, M.G. Hubbard, A model for gas-liquid slug flow in horizontal and near horizontal tubes, Ind. Eng. Chem. Fundam. 14 (4) (1975) 337–347 Nov..
[61] D. Barnea, N. Brauner, Holdup of the liquid slug in two phase intermittent flow, Int. J. Multiph. Flow 11 (1) (1985) 43–49 Jan..
[62] J. Fabre, A. Line, Modeling of two-phase slug flow, Annu. Rev. Fluid Mech. 24 (1) (1992) 21–46 Jan..
[63] O.J. Nydal, S. Pintus, P. Andreussi, Statistical characterization of slug flow in horizontal pipes, Int. J. Multiph. Flow 18 (3) (1992) 439–453 May.
[64] Y.D. Baba, A.M. Aliyu, A.E. Archibong, M. Abdulkadir, L. Lao, H. Yeung, Slug length for high viscosity oil-gas flow in horizontal pipes: experiments and prediction, J. Pet. Sci. Eng. 165 (2018).
[65] L. Norris, "Correlation of prudhoe bay liquid slug lengths and holdups including 1981 large diameter flow line tests," Houston, USA, 1982.
[66] J.P. Brill, Z. Schmidt, W.A. Coberly, J.D. Herring, D.W. Moore, Analysis of two-phase tests in large-diameter flow lines in prudhoe bay field, Soc. Pet. Eng. 21 (03) (1981).
[67] I. C. Gordon and P. C. Fairhurst, "Multi-phase pipeline and equipment design for marginal and deep water field development," in 3rd International Multiphase Flow Conference, 1987, pp. 1–12.
[68] S.L. Scott, O. Shoham, J.P. Brill, Prediction of slug length in horizontal, large-diameter pipes, Soc. Pet. Eng. 4 (3) (1989).